13th World Conference on Earthquake Engineering
Vancouver, B.C., Canada
August 1-6, 2004
Paper No. 1145

MODELING OF PHASE CHARACTERISTICS OF VERTICAL GROUND MOTION

Tomohiro KAWANISHI[1], Yoshitaka MURONO[1]

SUMMARY

In this study, we model the phase characteristics of vertical ground motion based on the concept of group delay time. For this purpose, we first calculate the average group delay time and its standard deviation by using the data of observed vertical ground motion, and then obtain the regression equations of these values as the functions of earthquake magnitude and epicentral distance. After that, we simulate sample vertical earthquake motions by using simulated phase spectra. Finally, we implement response analysis to investigate how the vertical ground motion influences the response of structure.

INTRODUCTION

Several studies have shown that the phase spectrum of an earthquake motion controls its non-stationary characteristics (Katsukura and Izumi, 1983)[1]. To investigate the non-stationary characteristics of earthquake motion, its phase characteristics should properly be modeled. We have modeled the phase characteristics of horizontal earthquake motion (Sato *et al.*, 1999)[2]. However, the phase spectrum of vertical ground motion has not been clarified yet. In this paper, we first derive regression equations for the mean and standard deviation of group delay time by using the observed vertical earthquake motion and simulate the vertical earthquake motion based on the regression equations. Finally, we investigate the effect of vertical ground motion on the response of structure by earthquake response analysis while taking into account the simulated vertical ground motions.

DATA USED FOR ANALYSIS

Table 1 shows the data used for regression analysis. We selected 57 vertical earthquake motions observed during five earthquakes, which are the same earthquakes as those we used for modeling the phase characteristics of horizontal ground motion.

[1] Railway Technical Research Institute, Tokyo, Japan

Table 1: Earthquake records used for analyses

Earthquake	M Magnitude	Number of records
Hokkaido Nansei-oki EQ (1993)	7.8	5
Hokkaido Toho-oki EQ (1994)	8.1	20
Sanriku Haruka-oki EQ (1994)	7.5	10
Hyogoken Nanbu EQ (1995)	7.2	7
Kagoshimaken Hokuseibu EQ (1997)	6.3	15

ANALYTICAL METHOD

Definition of Group Delay Time

The group delay time[3] is defined by the derivative of Fourier phase spectrum $\phi(\omega)$ with respect to the circular frequency ω as

$$t_{gr}(\omega) = \frac{d\phi(\omega)}{d\omega} \tag{1}$$

The mean value of the group delay time within a certain frequency band of which the central frequency is ω expresses the arrival time of a wave component at the frequency of ω. The standard deviation of the group delay time is related to the duration of the wave component. In view of these characteritics, we use the group delay time to model the phase spectrum.

Average Group Delay Time and Its Standard Deviation

To show the non-stationary characteristics of earthquake motion in the time and frequency domains, wavelet analysis is often used because the resolution in the time and frequency domains is guaranteed by the uncertainty criterion. Although there are several ways to define the analyzing wavelet $\varphi(t)$, we used the method of Meyer[4] to compose $\varphi(t)$. The Fourier transformation of $\varphi(t)$ has a compact support for each scale factor j (named the j-th compact support) defined by

$$\{2^j / 3T_d \le f \le 2^{j+2} / 3T_d\} \tag{2}$$

in which T_d is the duration of earthquake motion.

For all observed earthquake motions at sampling intervals of 0.01 (sec), we added zero data until the total number of sampling data of each earthquake motion N reach 131,072(=2^{17}). By using the wavelet transformation of each earthquake motion $x(t)$, we decomposed each time history of earthquake motion to a component time history of each scale factor j (j=0-16). We call it the j-th component time history $x^{(j)}(t)$. We calculate the mean $\mu_{tgr}^{(j)}$ and standard deviation $\sigma_{tgr}^{(j)}$ of group delay time of $x^{(j)}(t)$ on the j-th compact support by Eqs. (3) and (4):

$$\mu_{tgr}^{(j)} = \sum_{i=1}^{N^{(j)}} \frac{t_{gr}^{(j)}(\omega_i)}{N^{(j)}} \tag{3}$$

$$\sigma_{tgr}^{(j)} = \sqrt{\frac{1}{N^{(j)}} \sum_{i=1}^{N^{(j)}} \left(t_{gr}^{(j)}(\omega_i) - \mu_{tgr}^{(j)}\right)^2} \tag{4}$$

in which $N^{(j)}$ is the number of the data on the j-th compact support, and $t_{gr}^{(j)}(\omega)$ is the group delay time of the j-th component time history at the circular frequency of ω_i defined by

$$t_{gr}^{(j)}(\omega) = \frac{d\phi^{(j)}(\omega)}{d\omega} = -\frac{\phi^{(j)}(\omega_i) - \phi^{(j)}(\omega_{i+1})}{\Delta\omega} \tag{5}$$

The calculated Fourier phase spectrum $\phi^{(j)}(\omega)$ defined as a principal value within the range $[-\pi, \pi]$, therefore, we must unlap it to obtain the group delay time based on Eq. (5). We applied the method of Sawada *et al*[5] to unlap $\phi^{(j)}(\omega)$.

MODELING OF PROBABILISTIC CHARACTERISTICS OF GROUP DELAY TIME

We calculated the mean group delay time $\mu_{tgr}^{(j)}$ and its standard deviation $\sigma_{tgr}^{(j)}$ for all observed earthquake motions shown in **Table 1**. Because the trigger time of each earthquake motion is recorded and the rupture stating time is given, we shifted the origin time of each earthquake motion to the rupture stating time. The concerned period range in the standard aseismic design procedure is 0.1-5 sec. Therefore, the regression analyses of $\mu_{tgr}^{(j)}$ and $\sigma_{tgr}^{(j)}$ were conducted for $j = 7-14$.

We conducted regression analyses by using two parameters, the magnitude M and the epicentral distance Δ, by Eqs. (6) and (7):

$$\mu_{tgr}^{(j)} = \alpha_1^{(j)} \times 10^{\beta_1^{(j)}M} \times \Delta^{\gamma_1^{(j)}} \tag{6}$$

$$\sigma_{tgr}^{(j)} = \alpha_2^{(j)} \times 10^{\beta_2^{(j)}M} \times \Delta^{\gamma_2^{(j)}} \tag{7}$$

in which α, β and γ are the coefficients of regression equations obtained by regression analyses for the j-th component time history of earthquake motion. **Table 2** shows the results of regression analyses. The correlation coefficients for $\mu_{tgr}^{(j)}$ are larger than 0.90 for all scales j, and the correlation coefficients for $\sigma_{tgr}^{(j)}$ are 0.72 - 0.93.

SIMULATION OF EARTHQUAKE MOTIONS

To show the effectiveness of the obtained regression equations, we simulate earthquake motions by using the proposed group delay time model. At first, the values of $\mu_{tgr}^{(j)}$ and $\sigma_{tgr}^{(j)}$ on the j-th compact support are obtained from Eqs. (6) and (7). A sample group delay time $t_{gr}^{(j)}(\omega)$ on the j-th compact support is simulated by generating a random value based on the normal distribution $N(\mu_{tgr}^{(j)}, \sigma_{tgr}^{(j)})$. The phase spectrum $\phi^{(j)}(\omega)$ is obtained by integrating the group delay time with respect to the circular frequency. We decide the Fourier amplitude $A^{(j)}(\omega)$ as the simulated earthquake motion is compatible with the given response spectrum.

Figure 1 shows the simulated vertical ground motions for earthquake at the magnitude of 7.0 and three epicentral distances (30, 50 and 100km). We simulated vertical earthquake motions by using the response spectrum proposed by Kawashima *et al*[6]. The simulated earthquake motions have mainly high-frequency components first, which gradually change to low-frequency components as time passes by. The arrival time of the earthquake motion delays and the duration of the earthquake motion becomes longer as the epicentral distance becomes longer. **Figure 2** shows the horizontal ground motions simulated by the same method to use the horizontal group delay time model[2].

EFFECTS OF VERTICAL GROUND MOTIONS ON THE RESPONSE OF STRUCTURES

We clarify the effects of vertical ground motions on the response of structures by using two types of nonlinear model, a horizontal single degree of freedom model and a rocking single degree of freedom model. The equation of motion of the horizontal single degree of freedom model is defined by Eq. (8).

$$\ddot{x} + 2\xi\left(\frac{2\pi}{T}\right)\dot{x} + \frac{k(x)}{m} = \ddot{X} \tag{8}$$

Table 2: Regression coefficients

j	Range of frequency [Hz]	$\mu_{tgr}^{(j)}$			Correlation coefficient	$\sigma_{tgr}^{(j)}$			Correlation coefficient
		$\alpha_1^{(j)}$	$\beta_1^{(j)}$	$\gamma_1^{(j)}$		$\alpha_2^{(j)}$	$\beta_2^{(j)}$	$\gamma_2^{(j)}$	
7	0.033-0.130	0.612	0.031	0.440	0.936	8.596	0.0	0.440	0.728
8	0.065-0.260	0.339	0.105	0.357	0.955	1.215	0.133	0.357	0.800
9	0.130-0.521	0.582	0.112	0.175	0.956	0.458	0.232	0.175	0.800
10	0.260-1.042	0.799	0.085	0.255	0.971	1.765	0.108	0.255	0.739
11	0.521-2.083	1.226	0.020	0.365	0.991	1.450	0.098	0.365	0.815
12	1.042-4.167	0.745	0.041	0.317	0.991	0.587	0.125	0.317	0.875
13	2.083-8.333	0.493	0.055	0.350	0.992	0.264	0.160	0.350	0.925
14	4.167-16.667	0.369	0.063	0.396	0.992	0.152	0.184	0.396	0.892

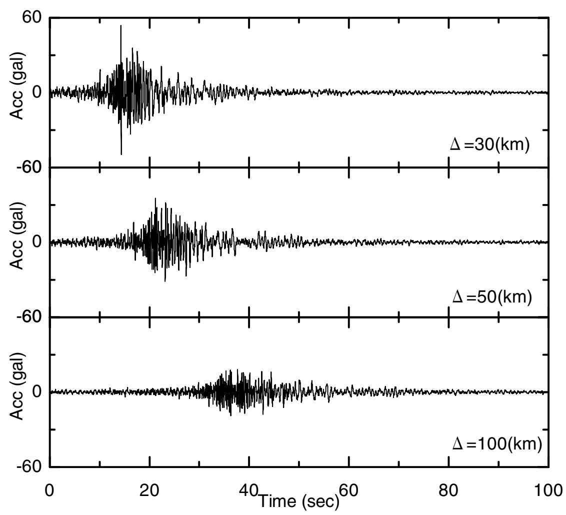

Figure 1 Simulated vertical ground motions

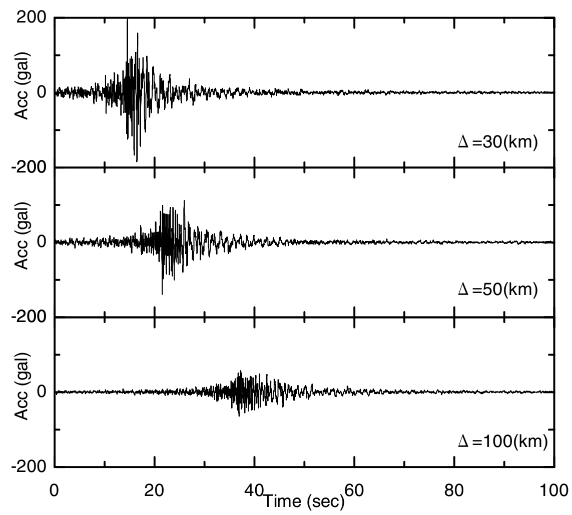

Figure 2 Simulated horizontal ground motions

in which m expresses the mass; ξ the damping factor and T the natural period. On the other hand, the equation of motion of the rocking single degree of freedom model that takes the P-Δ effect into account is defined by Eq. (9) as proposed by Yamashita *et al*[7].

$$\ddot{\phi} + 2\xi\left(\frac{2\pi}{T}\right)\dot{\phi} + \frac{M(\phi)}{mH^2} = -\frac{\ddot{X}}{H}\cos\phi + \frac{g+\ddot{Y}}{H}\sin\phi \tag{9}$$

in which $M(\phi)$ expresses the restoring moment; ϕ the angle of rotation of the pier; H the height of a pier and g the gravitational acceleration. We can take into account both the horizontal ground motion and the vertical ground motion by using a rocking model.

Figure 3 compares the displacement response calculated by using a horizontal model and the displacement response calculated by using a rocking model for the yielding strength of 0.2 and the height of a 5m-pier. In this calculation, we used the restoring moment characteristic expressed by a bilinear model and earthquake motions shown in **Figs. 1** and **2** for the epicentral distance of 50km. The peak value of the input horizontal acceleration was adjusted to 750 (gal), and that of the input vertical acceleration is also adjusted as the ratio of the peak vertical acceleration to the peak horizontal acceleration did not

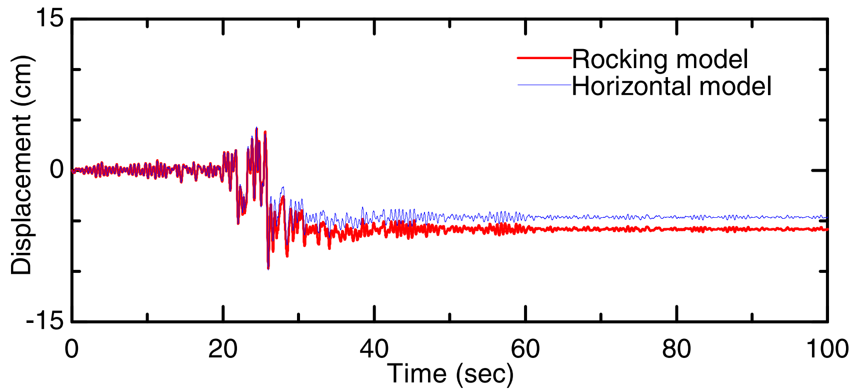

Figure 3 Comparison of the displacement response calculated by using a horizontal model and the displacement response calculated by using a rocking model

change. **Figure 3** indicates that the residual displacement in the rocking model is larger than that in the horizontal model.

Figure 4 compares the peak response displacement calculated by using the simulated earthquake motions and the peak response displacement calculated by using the observed earthquake motions. The horizontal axis expresses the peak value of the input horizontal acceleration, and the vertical axis expresses the peak response displacement. If the epicentral distance is short, the response displacement in the rocking model is larger than the peak response displacement in the horizontal model. Since the epicentral distance is longer, however, the peak response displacements in the two models become almost the same. This characteristic is applicable to both the response analyses to use the simulated earthquake motions and the response analyses to use the observed earthquake motions. This results show that the proposed phase spectrum model is effective for the simulation of vertical earthquake motions.

CONCLUDING REMARKS

We proposed a phase spectrum model of vertical ground motions by applying the concept of group delay time. By using two parameters, the magnitude M and the epicentral distance Δ, we derived the regression equations for the mean of group delay time and its standard deviation on compact supports of the Meyer wavelet. We checked the effectiveness of this phase spectrum model by simulating earthquake motions. We showed the effect of the simulated vertical ground motion on the response of structures by conducting response analyses with a rocking single degree of freedom model.

REFERENCES

1. Katsukura, K and Izumi, M. A fundamental study on the phase properties of seismic waves, *Journal of Structural and Construction Engineering, Transactions of AIJ.* No. 327, 20-27, 1983 (in Japanese).
2. Sato, T., Murono, Y., and Nishimura, A., Modeling of Phase Spectrum to Simulate Design Earthquake Motion, *Optimizing Post-Earthquake Lifeline System Reliability, Technical Council on Lifeline Earthquake Engineering, ASCE*, Monograph No. 16, 804-813, 1999.
3. Papoulis, A. The Fourier integral and its application, *McGraw-Hill*, 1962.
4. Meyer, Y., Orthonormal Wavelets, *in Wavelets*, Springer, 21-27, 1989.

5. Sawada, S., Morikawa, H., Toki, K., and Yokoyama, K., Identification of path and local site effects on phase spectrum of seismic motion, *Proceeding of 10th Japan Earthquake Engineering Symposium*, 915-921, 1998 (in Japanese).
6. Kawashima, K., Aizawa, K., Takahashi, K., Attenuation of peak ground motions and absolute acceleration response spectrum, *Report of Public Works Research Institute Ministry of Construction*, No. 166, 1985 (in Japanese).
7. Yamashita, N., Hata, Y, Harada, T., Takeuchi, S., Tanaka, H., Study on non-linear response analysis by considering large deformation due to P-Δ on SDOF model, *Proceeding of 11th Japan Earthquake Engineering Symposium (CD-ROM)*, 2002 (in Japanese).

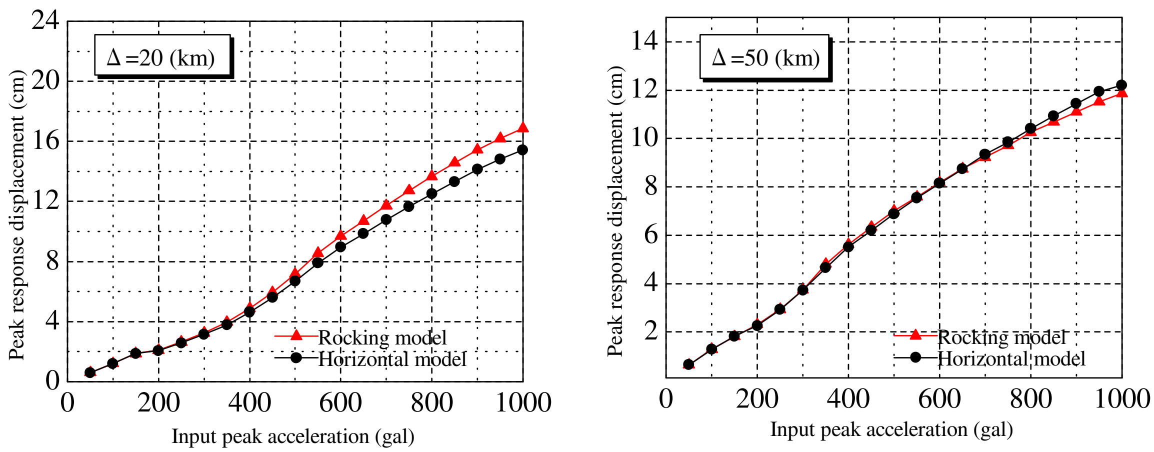

(a) Simulated earthquake motions

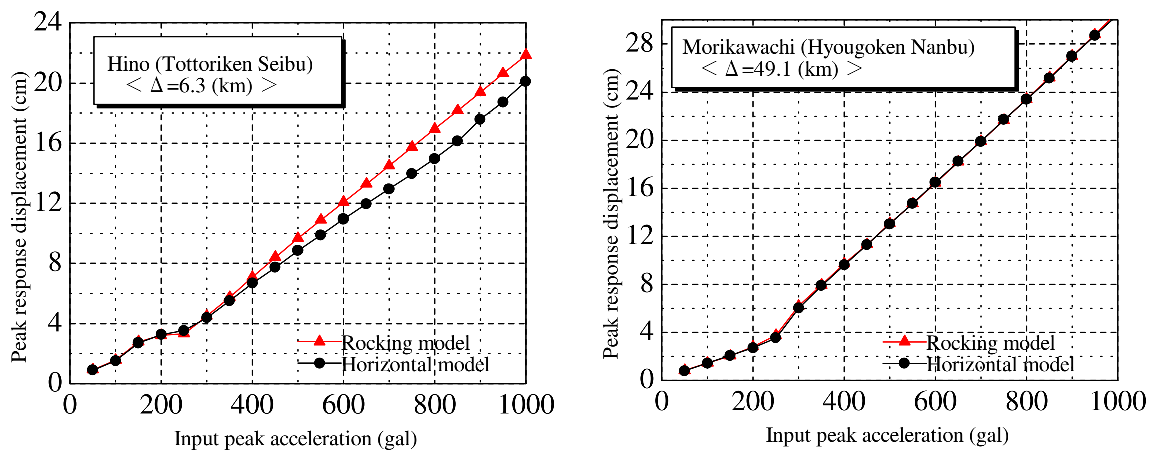

(b) Observed earthquake motions

Figure 4 Comparison of the response displacement calculated by using simulated earthquake motions and the response displacement calculated by using observed earthquake motions